metals

MDPI

Communication

Strain Rate Dependence of Twinning Behavior in AZ31 Mg Alloys

Jing Xu [1], Bo Guan [1,*], Xiaojun Zhao [2,*], Rui Fu [3], Qiang Hu [1] and Chaoqiang Liu [4,*]

[1] Institute of Applied Physics, Jiangxi Academy of Sciences, Nanchang 330029, China; jingxu1016@163.com (J.X.); huqiang1225@163.com (Q.H.)
[2] Key Laboratory of Advanced Technologies of Materials, Ministry of Education, Southwest Jiaotong University, Chengdu 610031, China
[3] International Joint Laboratory for Light Alloys, College of Materials Science and Engineering, Chongqing University, Chongqing 400030, China; fr@cqu.edu.cn
[4] State Key Laboratory of Powder Metallurgy, Central South University, Changsha 410083, China
* Correspondence: bguan2022@163.com (B.G.); xiaojunzhao@swjtu.edu.cn (X.Z.); liuchaoqiang@csu.edu.cn (C.L.)

Abstract: This study investigates the impact of strain rate on the twinning process (i.e., twin nucleation, twin propagation, and twin growth) and associated mechanical behavior during compression along the normal direction (ND) and transverse direction (TD) of a rolled AZ31 Mg plate at a range of strain rates from 0.00005 s^{-1} to 2500 s^{-1}. The findings reveal that the yield strength is insensitive to strain rates below 0.05 s^{-1} during both ND and TD compression tests, while at higher strain rates of 2500 s^{-1}, the yield strength increases under both loading conditions. Interestingly, the TD-compressed sample exhibits a larger yield plateau at a strain rate of 2500 s^{-1}, attributed to an increased activation of $\{10\bar{1}2\}$ twins. Further examination of the microstructure reveals that the twinning process is highly dependent on the strain rate. As the strain rate increases, twin nucleation is promoted, leading to a higher twin boundary density. In contrast, at lower strain rates, twin nucleation is restrained, and the external strain is mainly accommodated by twin growth, which results in higher area fractions of twinned regions.

Keywords: Mg alloys; strain rate; twinning; texture

check for updates

Citation: Xu, J.; Guan, B.; Zhao, X.; Fu, R.; Hu, Q.; Liu, C. Strain Rate Dependence of Twinning Behavior in AZ31 Mg Alloys. *Metals* **2023**, *13*, 1882. https://doi.org/10.3390/met13111882

Academic Editors: Sergey V. Zherebtsov and Frank Czerwinski

Received: 15 September 2023
Revised: 28 October 2023
Accepted: 10 November 2023
Published: 13 November 2023

Copyright: © 2023 by the authors. Licensee MDPI, Basel, Switzerland. This article is an open access article distributed under the terms and conditions of the Creative Commons Attribution (CC BY) license (https://creativecommons.org/licenses/by/4.0/).

1. Introduction

Magnesium (Mg) alloy has a lower density compared to steel and aluminum alloys, making it a promising material for replacing them in the automotive and aerospace industries [1–4]. Components in these industries often experience loading over a wide range of strain rates [5,6]. For instance, high-strain rate deformation occurs during automobile crashes or impacts [7,8]. Additionally, certain plastic forming technologies, such as explosive forming and electromagnetic forming, could exceed 10^3 s^{-1} in terms of strain rate [9–12]. Therefore, it is paramount to understand the plastic deformation behavior of Mg alloys at different strain rates [13].

To date, the mechanical performance and microstructural evolution of Mg alloys deformed at different strain rates have been extensively studied [14–16]. For example, Lin et al. [17] conducted a systematic study to investigate the effect of strain rate on the yield strength, ultimate tensile strength, and ductility of the extruded AZ31B Mg alloys. They found that the ultimate tensile strength and yield strength of the alloy increase with the strain rate, whereas the tensile ductility exhibits the opposite trend. Previous reports suggested that the dependence of mechanical properties and microstructure evolution on strain rate is associated with several parameters, such as deformation temperature, grain size and texture [18]. Texture plays a significant role in the variation of plastic deformation behavior with strain rate. Tucker et al. [19] reported that the yield strength of AZ31 Mg

alloys is highly affected by strain rate during compression along the normal direction (ND) of the plate, whereas it exhibited no strain rate dependence during compression along the transverse direction (TD) and rolling direction (RD). Hence, the strain rate sensitivity shows a substantial anisotropy in Mg alloys. The anisotropic strain rate sensitivity is strongly related to the activated deformation modes in certain conditions. Generally, Mg alloys show more significant strain rate sensitivity when the deformation is dominated by dislocation slip. A quantitative relationship between the activated deformation mode and mechanical properties is critical to understand the plastic deformation behavior of Mg alloys. Wang et al. [14] quantitatively studied the microstructure evolution during deformation at strain rates of 0.001, 1 and 600 s^{-1} in an AZ31 Mg alloy. They reported that the dislocation density of samples deformed at a strain rate of 600 s^{-1} is much higher than of samples deformed at a lower strain rate, while the $\{10\bar{1}2\}$ twin fraction increases remarkably with the strain rate, and is saturated when the strain rate is up to 1 s^{-1}. It is generally considered that the twinning process is characterized by twin nucleation, propagation and growth [20,21], as schematically shown in Figure 1. However, how the strain rate affects the twinning process is not yet clear. In addition, the critical resolved shear stress (CRSS) for twin nucleation and propagation is higher than that for twin growth, leading to the formation of a Lüders-like plateau in the stress-strain curves in some finer-grained samples. Given that strain rate has an important effect on twin activity, it would also affect the Lüders-like plateau. However, how strain rate affects the yield plateau also remains unclear.

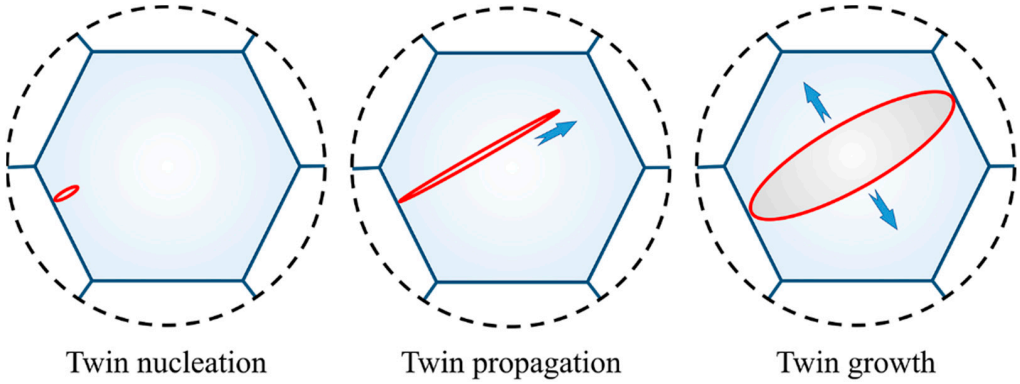


Figure 1. Schematic diagram on twin nucleation, propagation, and growth.

This study aims to quantitatively investigate the twinning process at different strain rates. To this end, a hot-rolled AZ31 Mg alloy followed by annealing were compressed at strain rate of 0.00005–2500 s^{-1}. The comprehensive analysis on deformation twins was conducted.

2. Experimental Procedure

An AZ31 Mg alloy in a hot-rolled state provided by Hebi Mgtu Technology Co., Ltd., (Hebi, China) was utilized as the initial material. The initial plate had dimensions of 10 mm (normal direction, ND) × 100 mm (transverse direction, TD) × 300 mm (rolling direction, RD). The specimens for compression test were cylinders with a height and diameter of 6 mm, cut from the edge of plate. Then, samples were annealed at 450 °C for 1 h. The compression tests were performed using a Split Hopkinson Pressure Bar system (SHPB) at a strain rate of 2500 s^{-1}. For the tests at a lower strain rate, an MTS machine (200 kN) was employed. Three samples were tested for each condition. Electron backscattered diffraction (EBSD) detector installed in a scanning electron microscopy (SEM, Tescan MIRA3, Brno, Czech Republic) was used to examine the microstructure of the samples. The samples for EBSD observation were mechanically ground using SiC paper, and then electron-chemically polished in a nitric acid and alcohol solution with a voltage of 20 V.

3. Results and Discussion

Figure 2 displays the microstructure of the annealed AZ31 Mg alloys. The average grain size is approximately 17 μm, and the annealed AZ31 Mg plate presents a strong basal texture with a maximum texture strength of 9.3, with most grains possessing a <*c*> axis parallel to the ND of the plate, as shown in Figure 2a. Beyerlein et al. [22] reported that the twinning process in Mg alloys is highly dependent on the texture or loading direction, as it is related to the Schmid factor. Specifically, the orientation relationship between two neighboring grains has a significant influence on the process of twin nucleation and growth, wherein decreasing the misorientation angle between neighboring grains leads to an increase in twin nucleation events that subsequently yield adjoining twin pairs. Furthermore, Beyerlein et al. [22] demonstrated that the thickest twins possess the highest Schmid factors, wherein 47% of twins have the highest Schmid factors in grains. It is generally accepted that $\{10\bar{1}2\}$ twinning predominates plastic deformation during compression along the transverse direction (TD) or rolling direction (RD) of a rolled plate, whereas the activity of $\{10\bar{1}2\}$ twinning is dramatically reduced during compression along the normal direction (ND). For a rolled plate with a strong peak of (0002) poles close to the ND, the plastic deformation behavior along the TD and RD is similar. Thus, to study the effect of strain rate on twinning of Mg alloys with different textures in a wide range of strain rates, a comparative study of the twinning behavior during compression along TD and ND was conducted, as depicted in Figure 2b.

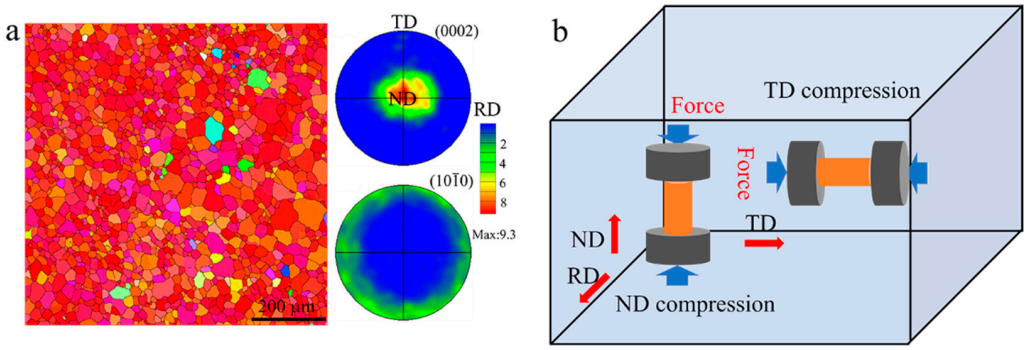


Figure 2. (**a**) Crystal orientation map of AZ31 plate and corresponding pole figure, (**b**) a schematic diagram showing the loading direction.

Figure 3 illustrates the true stress-strain curves of AZ31 plate during compression along TD and ND at different strain rate. For TD compression (Figure 3a), all curves exhibit a sigmoidal shape, which is typical feature of plastic deformation dominated by $\{10\bar{1}2\}$ twinning. A region with constant stress in the strain-stress curves is observed, which forms a yield plateau (Lüders-like plateau). The strain of yield plateau is about 0.014, 0.0041 and 0.0026 at strain rate of 2500 s^{-1}, 0.05 s^{-1} and 0.00005 s^{-1}, respectively. For ND compression (Figure 3b), the stress-strain curves exhibit a common parabolic shape. The yield strength of samples under TD compression is 67 ± 2 MPa, 67 ± 3 MPa, 75 ± 2 MPa at strain rate of 0.00005 s^{-1}, 0.05 s^{-1} and 2500 s^{-1}, which is approximately 109 ± 1 MPa, 110 ± 3 MPa, and 145 ± 5 MPa of samples under ND compression, respectively. Apparently, the yield strength for both TD and ND compression is similar at a strain rate of 0.00005 s^{-1} and 0.05 s^{-1}, and it increases at a strain rate of 2500 s^{-1}.

Figure 4 displays the microstructure of AZ31 plates after compression along ND and TD to about 3–4% strain. The black lines mark the high-angle grain boundaries with a misorientation angle over 15°, and the red lines indicate the $\{10\bar{1}2\}$ twin boundaries. For compression along the ND, the $\{10\bar{1}2\}$ twin fraction increases with the strain rate. However, the fraction of all samples remains low, which indicates that slip is the predominant deformation mode during ND compression. In contrast, the twin fraction for TD compression is remarkably higher than that for ND compression. It is observed that the fraction of twinned regions and the number of twin boundaries in each grain increases with the strain rate. In

this study, the number of twin boundaries in each grain is calculated, and the statistical results are shown in Figure 5 (it is considered that a twin consists of two twin boundaries). The grains with more than five twin boundaries account for approximately 87% of the sample deformed at a strain rate of 2500 s^{-1}, which is around 36% of the sample deformed at a strain rate of 0.00005 s^{-1}. Additionally, the average number of twin boundaries per grain increases with the strain rate, ranging from 3.4 to 5.6 and 6.3 in the samples defamed at a strain rate of 0.00005 s^{-1}, to 0.05 s^{-1} and 2500 s^{-1}, respectively.

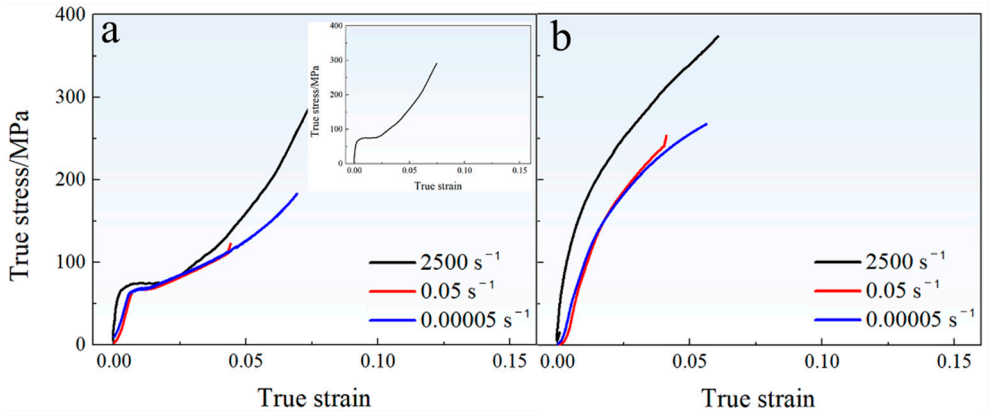


Figure 3. True stress-strain curves of the AZ31 plates: (**a**) under compression along transverse direction (TD), (**b**) under compression along normal direction (ND).

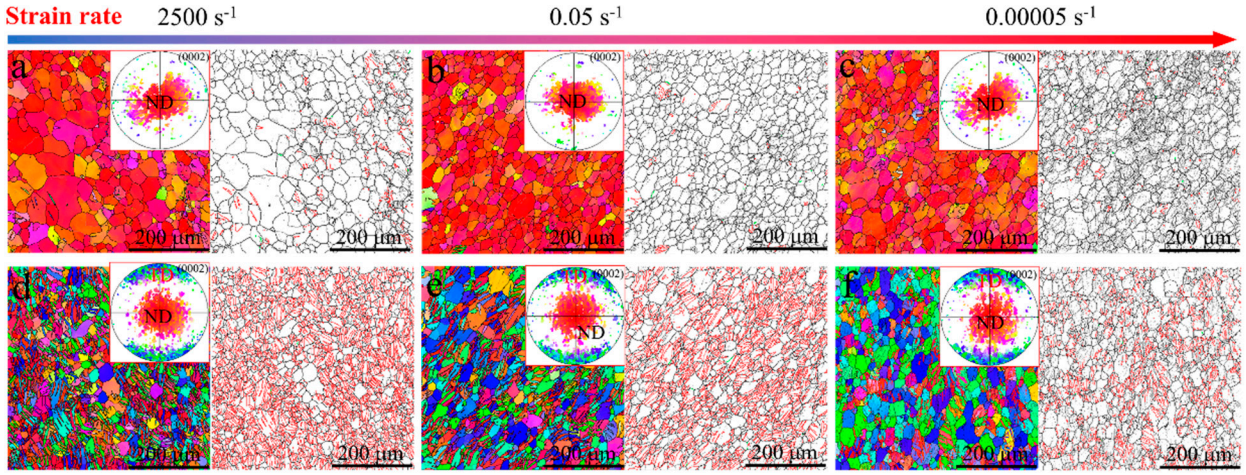


Figure 4. Crystal orientation map and {10$\bar{1}$2} twin boundary distribution of AZ31 plate after compression to 3–4% strain: (**a**–**c**) under ND compression at strain rate of 2500 s^{-1}, 0.05 s^{-1}, and 0.00005 s^{-1}, respectively, (**d**–**f**) under TD compression at strain rate of 2500 s^{-1}, 0.05 s^{-1}, and 0.00005 s^{-1}, respectively.

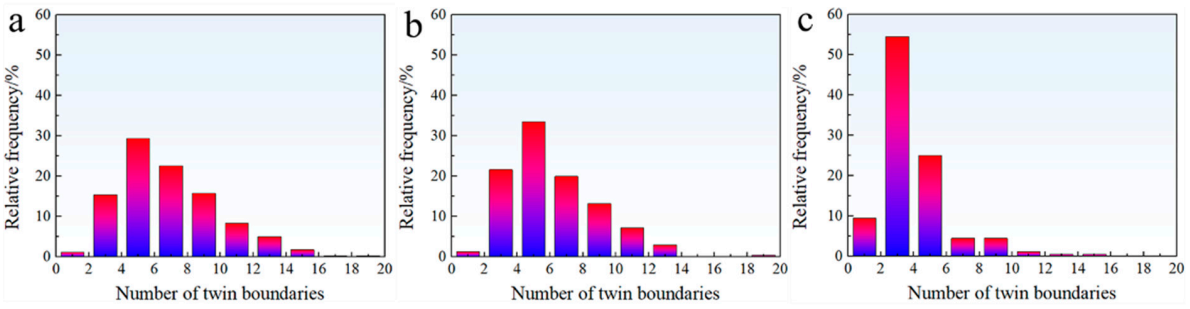


Figure 5. Frequency of twin boundaries in each grain under compression along TD: (**a**–**c**) at strain rate of 2500 s^{-1}, 0.05 s^{-1}, and 0.00005 s^{-1}.

For the Mg alloy, {10$\bar{1}$2} twinning could cause a reorientation of the *c*-axis of parent grains by 86° around the <1$\bar{2}$10> axis, leading to a dramatic change in texture, as depicted by the pole figures in Figure 4. Figure 6 shows the crystal orientation maps of the twinned region for the AZ31 plates after TD compression and ND compression. The area fraction of the twinned region is calculated and listed in Table 1. For ND compression, the area fraction of the twinned region increases from 0.2% to 0.5% and 1.1% as the strain rate increases from 0.00005 s^{-1}, to 0.05 s^{-1} and 2500 s^{-1}. For TD compression, the area fraction is 48.2%, 61.1% and 80.1% at strain rates of 2500 s^{-1}, 0.05 s^{-1} and 0.00005 s^{-1}, respectively. As shown in Figure 6, parts of grains are completely twinned after TD compression to 3–4% strain, and the number of completely twinned grains at different strain rate is 25, 47 and 136 at strain rates of 2500 s^{-1}, 0.05 s^{-1} and 0.00005 s^{-1}, respectively (listed in Table 2).

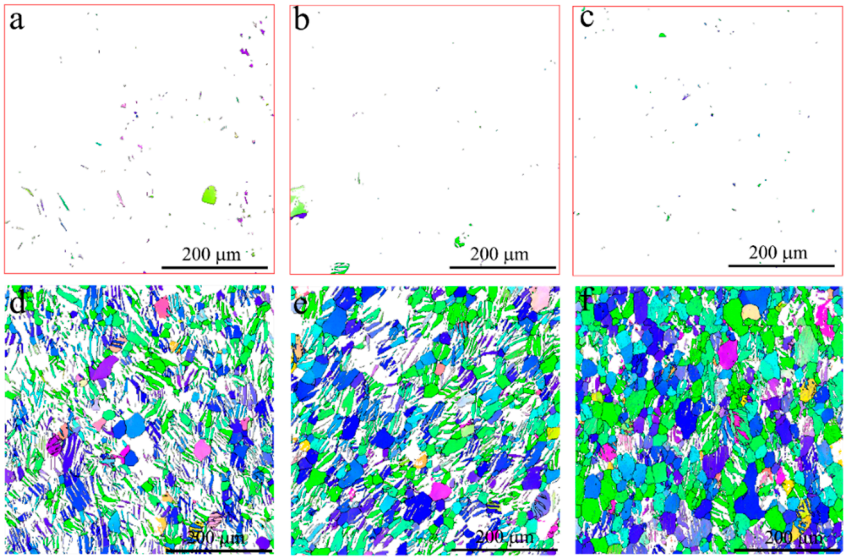


Figure 6. Crystal orientation map of twinned region, (**a–c**): under ND compression at strain rate of 2500 s^{-1}, 0.05 s^{-1}, and 0.00005 s^{-1}, respectively, (**d–f**) under TD compression at strain rate of 2500 s^{-1}, 0.05 s^{-1}, and 0.00005 s^{-1}.

Table 1. Area fraction of twinned region for ND compression and TD compression.

Loading direction	2500 s^{-1}	0.05 s^{-1}	0.00005 s^{-1}
ND compression	1.2%	0.5%	0.2%
TD compression	48.2%	61.1%	80.1%

Table 2. Number of grains being completely twinned after TD compression.

Loading direction	2500 s^{-1}	0.05 s^{-1}	0.00005 s^{-1}
TD compression	25	47	136

As shown in Figure 2, the yield strength for TD and ND compression at a strain rate of 2500 s^{-1} is higher compared to that at lower strain rates. Wang et al., conducted a study on the evolution of mechanical properties, dislocation and twin densities in Mg alloys deformed at different strain rates [14]. Their results suggest that the increment in yield strength with strain rate is primarily attributed to the variation of dislocation density. During ND compression, basal slip is the dominant deformation mode for rolled Mg alloy, which has been confirmed through slip trace analysis by Xu et al. [23]. A higher strain rate would lead to an increase in yield strength due to the dependence of dislocation slip on strain rate. {10$\bar{1}$2} twinning would dominate the plastic deformation during TD compression. However, it is generally accepted that the critical resolved shear stress for

{10$\bar{1}$2} twinning is insensitive to strain rate. Hence, an unexpected enhancement of yield strength under TD compression at a higher strain rate appears. A similar enhancement of yield strength for the twinning-dominated deformation condition was also reported by Shen et al. [24]. The mechanical properties of materials are closely related to their deformation modes [25–27]. In this study, the activities of basal <a> slip, prismatic <a> slip, and {10$\bar{1}$2} twinning under TD compression are calculated. The calculation was performed based on the following steps [28,29]. First, the Euler angles in the crystal orientation maps in Figure 2 were exported in Channel 5 software (Oxford Instruments, Abingdon, UK). Then, the Schmid factor of each slip system or twinning system is calculated. The activated deformation mode for each Euler angle is determined by comparing the activation stress for each slip/twinning system, and the one with the lowest activation stress is operated during loading. The activation stress for each mode is determined by both critical resolved shear stress (CRSS) and Schmid factor (m) as follows: $\sigma = \mathrm{CRSS}/m$. For Mg alloys, it is hard to experimentally determine the CRSS value for each deformation mode due to the high sensitivity of CRSS to grain size, deformation temperature and alloying elements. It is generally considered that the CRSS for basal slip is the lowest, and the CRSS for {10$\bar{1}$2} twinning is higher than that of basal slip but lower than that of prismatic slip [23,30–32]. Therefore, two typical CRSS ratios of 1:1:3 and 1:2:3 for basal slip: {10$\bar{1}$2} twinning: prismatic slip are used. The calculated results of the fraction of grains favoring basal slip, prismatic slip, and {10$\bar{1}$2} twinning using these two CRSS ratios are presented in Figure 7. It is worth noting that, due to the lower Schmid factor under TD compression and higher CRSS of prismatic slip, the fraction of prismatic slip in both calculations is 0, which is not shown in Figure 7. For a CRSS ratio of 1:1:3, the fraction for {10$\bar{1}$2} twinning and basal slip is approximately 72.7% and 27.3%, respectively. For a CRSS ratio of 1:2:3, the fraction of {10$\bar{1}$2} twinning is about 45.8%, and that for basal slip is about 54.2%. These results demonstrate that basal slip is also an important deformation mode of the Mg plate for TD compression. The results are consistent with the findings on the activity of the deformation mode for the AZ31 Mg plate under TD compression reported by Yu et al. [33]. Thus, due to the activation of basal slip, an unexpected enhancement of yield strength under TD compression at a strain rate of 2500 s^{-1} occurs due to the dependence of dislocation slip on strain rate.

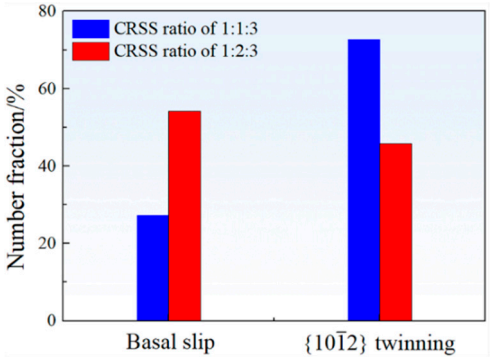


Figure 7. Number fraction of grains favoring basal slip and {10$\bar{1}$2} twinning under TD compression with CRSS ratio of 1:1:3 and 1:2:3 of basal slip, {10$\bar{1}$2} twinning, and prismatic slip.

From Figures 4–6, the area fraction for the twinned region decreases with increasing strain rate during TD compression. This phenomenon can be attributed to the effect of texture and strain rate on the twinning process. During deformation, a twin nucleates at a boundary and immediately propagates along the twinning direction on the twinning plane until it reaches the boundary on the other side of the grain. Wu et al. [20] considered that the thickness of the twinned region does not increase significantly at the end of propagation. Hence, twin nucleation and propagation effectively increase the twin boundary density, whereas they have a minor impact on increasing the arear fraction of the twinned region. For the twin growth process, twin dislocation glides in the matrix on the twin boundary, leading to a significant increase in the twinned region. As shown in Figure 3, the yield

strength of the AZ31 Mg plate at a strain rate of 2500 s^{-1} is higher than that for other deformation conditions. However, the CRSS for $\{10\bar{1}2\}$ twinning is insensitive to strain rate. This would promote twin nucleation and enhance the twin boundaries effectively at a higher strain rate. At lower strain rate, twin nucleation is restrained, and external strain is accommodated by twin growth, resulting in the higher area fraction of twinned region during TD compression. For twinning process, the CRSS for twin nucleation and propagation is higher than that for twin growth. Due to the profuse twin nucleation at higher strain rate, a high-stress release is expected, leading to the formation of a yield plateau. Previously, the yield plateau was often observed for Mg alloys with finer grains during twinning-dominated conditions [34,35]. Matthew R. Barnett et al. [34] reported that AZ31 Mg alloy with fine grains (average grain size smaller than 15 μm) showed a yield plateau. The strain of the plateau decreases with increasing grain size and would disappear when the average grain size is larger than 55 μm. Further examination had shown that $\{10\bar{1}2\}$ twins would propagate from grain to neighboring grain over the sample during yielding, which could effectively release the stress, leading to the formation of a yield plateau. The results of this study show that such a yield plateau could be detected at high strain rates for samples with coarse grains as well.

4. Conclusions

The present study systematically investigated the influence of strain rate and texture on the plastic deformation behavior and microstructure evolution of a rolled AZ31 magnesium plate, along with the underlying mechanisms. The major findings are summarized as follows:

(a) The yield strength of AZ31 plates, when compressed along the transverse direction (TD) and normal direction (ND) at a strain rate of 0.00005 s^{-1}, is comparable to that obtained at a strain rate of 0.05 s^{-1}. However, an increase in yield strength is observed at a strain rate of 2500 s^{-1} due to the activation of the basal slip.

(b) The twinning process is strongly related to strain rate. Increasing the strain rate would promote twin nucleation, leading to a high twin boundary density for TD compression. At a lower strain rate, twin nucleation is limited; the external strain would be accommodated by twin growth, resulting in a higher area fraction of the twinned region.

(c) The formation of the yield plateau observed during TD compression is attributed to the twinning process. At a higher strain rate, a high number of twins are nucleated and a stress release of a large amount is expected, which would contribute to the formation of a yield plateau.

Author Contributions: Formal analysis, J.X., B.G., X.Z., R.F., Q.H. and C.L.; investigation, J.X., B.G., X.Z. and R.F.; data curation, J.X. and B.G.; writing—original draft preparation, J.X., B.G., X.Z. and C.L.; writing—review and editing, J.X., B.G., X.Z. and C.L.; funding acquisition, Q.H. All authors have read and agreed to the published version of the manuscript.

Funding: Bo Guan and Jing Xu were financially supported by the National Key Research and Development Program of China (No. 2022YFB3708400), National Natural Science Foundation of China (52301151), Jiangxi Provincial Natural Science Foundation (No. 20224BAB214017 and 20232BAB214002), Jiangxi Academy of Sciences (Nos. 2022YSBG22023, 2022YSBG22024). Xiaojun Zhao was financially supported by National Natural Science Foundation of China (52101150), Sichuan Science and Technology Program (2022YFG0287). Chaoqiang Liu was financially supported by National Natural Science Foundation of China (52101167).

Data Availability Statement: The data that support the findings of this study are available from the corresponding author upon reasonable request.

Conflicts of Interest: The authors declare that there is no conflict of interest.

References

1. Yan, C.; Xin, Y.; Chen, X.B.; Xu, D.; Chu, P.K.; Liu, C.; Guan, B.; Huang, X.; Liu, Q. Evading strength-corrosion tradeoff in Mg alloys via dense ultrafine twins. *Nat. Commun.* **2021**, *12*, 4616. [CrossRef] [PubMed]
2. Zeng, Z.; Nie, J.F.; Xu, S.W.; Hj Davies, C.; Birbilis, N. Super-formable pure magnesium at room temperature. *Nat. Commun.* **2017**, *8*, 972. [CrossRef] [PubMed]
3. Zhou, S.; Tang, A.; Liu, T.; Peng, P.; Zhang, J.; She, J.; Pan, F. Ductility enhancement by activating non-basal slip in as-extruded Mg alloys with dilute Sc addition. *J. Mater. Res. Technol.* **2023**, *22*, 3362–3374. [CrossRef]
4. Li, C.; Yan, H.; Chen, R. Microstructure and Texture Evolution of Mg-14Gd-0.5Zr Alloy during Rolling and Annealing under Different Temperatures. *Acta Metall. Sin.* **2022**, *36*, 61–76. [CrossRef]
5. Sunder Sharma, S.; Yadav, S.; Joshi, A.; Goyal, A.; Khatri, R. Application of metallic foam in vehicle structure: A review. *Mater. Today Proc.* **2022**, *63*, 347–353. [CrossRef]
6. Hong Hue, D.T.; Tran, V.K.; Nguyen, V.L.; Van Lich, L.; Dinh, V.H.; Nguyen, T.G. High strain-rate effect on microstructure evolution and plasticity of aluminum 5052 alloy nano-multilayer: A molecular dynamics study. *Vacuum* **2022**, *201*, 111104. [CrossRef]
7. Finfrock, C.B.; Bhattacharya, D.; McBride, B.N.L.; Ballard, T.J.; Clarke, A.J.; Clarke, K.D. Decoupling the Impacts of Strain Rate and Temperature on TRIP in a Q&P Steel. *JOM* **2022**, *74*, 506–512.
8. Smerd, R.; Winkler, S.; Salisbury, C.; Worswick, M.; Lloyd, D.; Finn, M. High strain rate tensile testing of automotive aluminum alloy sheet. *Int. J. Impact Eng.* **2005**, *32*, 541–560. [CrossRef]
9. Kurukuri, S.; Worswick, M.J.; Bardelcik, A.; Mishra, R.K.; Carter, J.T. Constitutive Behavior of Commercial Grade ZEK100 Magnesium Alloy Sheet over a Wide Range of Strain Rates. *Metall. Mater. Trans. A* **2014**, *45*, 3321–3337. [CrossRef]
10. Du, Z.; Cui, X.; Yang, H.; Xia, W. Deformation and fracture behavior of 5052 aluminum alloy by electromagnetic-driven stamping. *Int. J. Adv. Manuf. Technol.* **2022**, *123*, 3955–3968. [CrossRef]
11. Afrasiab, M.; Hojjat, Y.; Faraji, G.; Moslemi Naeini, H. Formability enhancement of ultrafine-grained pure copper sheets produced by accumulative roll bonding aided by electromagnetic forming. *Int. J. Adv. Manuf. Technol.* **2022**, *120*, 7445–7459. [CrossRef]
12. Shabanpour, M.; Arezoudar, A.F. Effect of layer lay-up on formability of Al–Cu two-layer sheet in electromagnetic forming. *Int. J. Adv. Manuf. Technol.* **2021**, *112*, 2773–2788. [CrossRef]
13. Wang, H.; Wu, P.; Kurukuri, S.; Worswick, M.J.; Peng, Y.; Tang, D.; Li, D. Strain rate sensitivities of deformation mechanisms in magnesium alloys. *Int. J. Plast.* **2018**, *107*, 207–222. [CrossRef]
14. Wang, M.; Xu, X.Y.; Wang, H.Y.; He, L.H.; Huang, M.X. Evolution of dislocation and twin densities in a Mg alloy at quasi-static and high strain rates. *Acta Mater.* **2020**, *201*, 102–113. [CrossRef]
15. Della Ventura, N.M.; Schweizer, P.; Sharma, A.; Jain, M.; Edwards, T.E.J.; Schwiedrzik, J.J.; Peruzzi, C.; Logé, R.E.; Michler, J.; Maeder, X. Micromechanical response of pure magnesium at different strain rate and temperature conditions: Twin to slip and slip to twin transitions. *Acta Mater.* **2023**, *243*, 118528. [CrossRef]
16. Yu, J.; Song, B.; Xia, D.; Zeng, X.; Huang, Y.; Hort, N.; Mao, P.; Liu, Z. Dynamic tensile properties and microstructural evolution of extruded EW75 magnesium alloy at high strain rates. *J. Magnes. Alloys* **2020**, *8*, 849–859. [CrossRef]
17. Lin, X.Z.; Chen, D.L. Strain Hardening and Strain-Rate Sensitivity of an Extruded Magnesium Al. *J. Mater. Eng. Perform.* **2008**, *17*, 894–901. [CrossRef]
18. Karimi, E.; Zarei-Hanzaki, A.; Pishbin, M.H.; Abedi, H.R.; Changizian, P. Instantaneous strain rate sensitivity of wrought AZ31 magnesium Al. *Mater. Des.* **2013**, *49*, 173–180. [CrossRef]
19. Tucker, M.; Horstemeyer, M.; Gullett, P.; Elkadiri, H.; Whittington, W. Anisotropic effects on the strain rate dependence of a wrought magnesium Al. *Scr. Mater.* **2009**, *60*, 182–185. [CrossRef]
20. Wu, P.D.; Guo, X.Q.; Qiao, H.; Lloyd, D.J. A constitutive model of twin nucleation, propagation and growth in magnesium crystals. *Mater. Sci. Eng. A* **2015**, *625*, 140–145. [CrossRef]
21. Wang, H.; Wu, P.D.; Wang, J.; Tomé, C.N. A crystal plasticity model for hexagonal close packed (HCP) crystals including twinning and de-twinning mechanisms. *Int. J. Plast.* **2013**, *49*, 36–52. [CrossRef]
22. Beyerlein, I.J.; Capolungo, L.; Marshall, P.E.; McCabe, R.J.; Tomé, C.N. Statistical analyses of deformation twinning in magnesium. *Philos. Mag.* **2010**, *90*, 2161–2190. [CrossRef]
23. Xu, J.; Guan, B.; Xin, Y.; Huang, G.; Wu, P.; Liu, Q. Revealing the role of pyramidal <c+a> slip in the high ductility of Mg-Li Al. *J. Magnes. Alloys* **2021**, in press.
24. Shen, J.; Kondoh, K.; Jones, T.L.; Mathaudhu, S.N.; Kecskes, L.J.; Wei, Q. Effect of strain rate on the mechanical properties of magnesium alloy AMX602. *Mater. Sci. Eng. A* **2016**, *649*, 338–348. [CrossRef]
25. Meng, Y.; Yu, J.; Zhang, G.; Wu, Y.; Zhang, Z.; Shi, Z. Effect of circumferential strain rate on dynamic recrystallization and texture of Mg-13Gd-4Y-2Zn-0.5Zr alloy during rotary backward extrusion. *J. Magnes. Alloys* **2020**, *8*, 1228–1237. [CrossRef]
26. Zhao, L.; Guan, B.; Xin, Y.; Huang, X.; Liu, C.; Wu, P.; Liu, Q. A quantitative study on mechanical behavior of Mg alloys with bimodal texture components. *Acta Mater.* **2021**, *214*, 117013. [CrossRef]
27. Zhang, Z.; Zhang, J.; Xie, J.; Liu, S.; Fu, W.; Wu, R. Developing a Mg alloy with ultrahigh room temperature ductility via grain boundary segregation and activation of non-basal slips. *Int. J. Plast.* **2023**, *162*, 103548. [CrossRef]
28. Guan, B.; Xin, Y.; Huang, X.; Liu, C.; Wu, P.; Liu, Q. The mechanism for an orientation dependence of grain boundary strengthening in pure titanium. *Int. J. Plast.* **2022**, *153*, 103276. [CrossRef]

29. Wen, Y.; Guan, B.; Xin, Y.; Liu, C.; Wu, P.; Huang, G.; Liu, Q. Solute atom mediated Hall-Petch relations for magnesium binary alloys. *Scr. Mater.* **2022**, *210*, 114451. [CrossRef]
30. Xu, J.; Guan, B.; Xin, Y.; Wei, X.; Huang, G.; Liu, C.; Liu, Q. A weak texture dependence of Hall–Petch relation in a rare-earth containing magnesium Al. *J. Mater. Sci. Technol.* **2022**, *99*, 251–259. [CrossRef]
31. Zhou, B.; Li, Y.; Wang, L.; Jia, H.; Zeng, X. The role of grain boundary plane in slip transfer during deformation of magnesium alloys. *Acta Mater.* **2022**, *227*, 117662. [CrossRef]
32. Li, T.; Zheng, J.; Xia, L.; Shou, H.; Zhang, Y.; Shi, R.; He, L.; Li, W. Tailoring Texture to Highly Strengthen AZ31 Alloy Plate in the Thickness Direction via Pre-tension and Rolling–Annealing. *Acta Metall. Sin.* **2022**, *36*, 266–280. [CrossRef]
33. Yu, H.; Li, C.; Xin, Y.; Chapuis, A.; Huang, X.; Liu, Q. The mechanism for the high dependence of the Hall-Petch slope for twinning/slip on texture in Mg alloys. *Acta Mater.* **2017**, *128*, 313–326. [CrossRef]
34. Barnett, M.R.; Nave, M.D.; Ghaderi, A. Yield point elongation due to twinning in a magnesium Al. *Acta Mater.* **2012**, *60*, 1433–1443. [CrossRef]
35. Zhou, S.; Liu, T.; Tang, A.; Huang, Y.; Peng, P.; Zhang, J.; Hort, N.; Willumeit-Römer, R.; Pan, F. Designing Mg alloys with high strength and ductility by reducing the strength difference between the basal and non-basal slips. *Mater. Des.* **2023**, *225*, 111476. [CrossRef]

Disclaimer/Publisher's Note: The statements, opinions and data contained in all publications are solely those of the individual author(s) and contributor(s) and not of MDPI and/or the editor(s). MDPI and/or the editor(s) disclaim responsibility for any injury to people or property resulting from any ideas, methods, instructions or products referred to in the content.